ST segment elevation by current-to-load mismatch: an experimental and computational study

Mark G. Hoogendijk, MD,* Mark Potse, PhD,*† Alain Vinet, PhD,‡§ Jacques M.T. de Bakker, PhD,*¶ Ruben Coronel, MD, PhD*

**From the Department of Experimental Cardiology, Heart Failure Research Center, Academic Medical Center, University of Amsterdam, Amsterdam, and †Cardiovascular Research Institute Maastricht, Maastricht University, Maastricht, The Netherlands, ‡Research Center, Sacré-Coeur Hospital, and §Institute of Biomedical Engineering, Université de Montréal, Montreal, Quebec, Canada, and ¶Interuniversity Cardiology Institute of The Netherlands, Utrecht, The Netherlands.*

BACKGROUND Recently, we demonstrated that ajmaline caused ST segment elevation in the heart of an *SCN5A* mutation carrier by excitation failure in structurally discontinuous myocardium. In patients with Brugada syndrome, ST segment elevation is modulated by cardiac sodium (I_{Na}), transient outward (I_{to}), and L-type calcium currents (I_{CaL}).

OBJECTIVE To establish experimentally whether excitation failure by current-to-load mismatch causes ST segment elevation and is modulated by I_{to} and I_{CaL}.

METHODS In porcine epicardial shavings, isthmuses of 0.9, 1.1, or 1.3 mm in width were created parallel to the fiber orientation. Local activation was recorded electrically or optically (di-4-ANEPPS) simultaneously with a pseudo-electrocardiogram (ECG) before and after ajmaline application. Intra- and extracellular potentials and ECGs were simulated in a computer model of the heart and thorax before and after introduction of right ventricular structural discontinuities and during varying levels of I_{Na}, I_{to}, and I_{CaL}.

RESULTS In epicardial shavings, conduction blocked after ajmaline in a frequency-dependent manner in all preparations with isthmuses $\leq$1.1 mm width. Total conduction block occurred in three of four preparations with isthmuses of 0.9 mm versus one of seven with isthmuses $\geq$1.1 mm ($P<.05$). Excitation failure resulted in ST segment elevation on the pseudo-ECG. In computer simulations, subepicardial structural discontinuities caused local activation delay and made the success of conduction sensitive to I_{Na}, I_{to}, and I_{CaL}. Reduction of I_{to} and increase of I_{CaL} resulted in a higher excitatory current, overcame subepicardial excitation failure, and reduced the ST segment elevation.

CONCLUSIONS Excitation failure by current-to-load mismatch causes ST segment elevation and, like ST segment elevation in Brugada patients, is modulated by I_{to} and I_{CaL}.

KEYWORDS Brugada syndrome; structure; ST segment elevation

ABBREVIATIONS **ECG** = electrocardiogram; **CACNA1C** = gene encoding the α_1 subunit of the L-type calcium channel; **CACNB2b** = gene encoding the β_{2b} subunit of the L-type calcium channel; $\mathbf{G_{Na}}$ = sodium channel conductivity; $\mathbf{G_{CaL}}$ = L-type calcium channel conductivity; $\mathbf{G_{to}}$ = transient outward conductivity; $\mathbf{I_{Na}}$ = sodium current; $\mathbf{I_{CaL}}$ = L-type calcium current; $\mathbf{I_{to}}$ = transient outward current; **SCN5A** = gene encoding the α subunit of the cardiac sodium channel

(Heart Rhythm 2011;8:111–118)

Introduction

Coved ST segment elevation followed by a negative T wave in the right precordial leads is the electrocardiographic (ECG) hallmark of the Brugada syndrome.[1] Thus far, no mechanism of this so-called Brugada ECG pattern has been demonstrated in patients.[2]

A reduced function of the cardiac sodium channel plays an important role in the mechanism of the Brugada syndrome: sodium channel blockers can provoke or augment the Brugada ECG pattern,[3] and loss-of-function mutations in *SCN5A*, the gene encoding the α-subunit of the cardiac sodium channel, are identified in ~20% of patients.[4] Additionally, structural discontinuities appear to play a role because subtle signs of right ventricular structural discontinuities are common in patients with Brugada syndrome.[2,5–8]

Recently, we demonstrated in the explanted heart of an *SCN5A* mutation carrier that sodium channel blockade caused excitation failure in discontinuous myocardium, which showed as ST segment elevation on a pseudo-ECG.[9] At sites at which structural discontinuities cause sudden expansion of the myocardium, more depolarizing current is required for cells to reach threshold potential, and conduction can fail especially if available excitatory current is reduced (current-to-load mismatch).[10,11] In addition, we demonstrated in a computer model that excitation failure and activation delay by current-to-load

The first two authors contributed equally to this work. This study was supported by the Netherlands Heart Foundation (2008B062 to RC) and by the Interuniversity Cardiology Institute of the Netherlands. Computational resources were provided by the Réseau Québécois de Calcul de Haute Performance. **Address reprint requests and correspondence:** Mark Hoogendijk, M.D., Heart Failure Research Center, Academic Medical Center, Meibergdreef 9, 1105 AZ, Amsterdam, The Netherlands. E-mail address: m.g.hoogendijk@amc.uva.nl. (Received August 3, 2010; accepted September 15, 2010.)

mismatch can result in the Brugada ECG pattern and concluded that current-to-load mismatch may underlie the Brugada ECG pattern.[9] However, a direct experimental proof that excitation failure by current-to-load mismatch results in ST segment elevation is still lacking.

The Brugada ECG pattern is modulated not only by cardiac sodium current (I_{Na}) but also by transient outward (I_{to}) and L-type calcium current (I_{CaL}). Quinidine, a class 1A sodium channel blocker that also blocks I_{to},[12] can ameliorate the ST segment elevation of the Brugada ECG pattern[13] and reduces inducibility of ventricular arrhythmias.[14] Likewise, pharmacological enhancement of I_{CaL} by isoproterenol can reduce the Brugada ECG pattern[3] and is applied to treat electrical storms.[15] Furthermore, mutations in *CACNA1C* and *CACNB2b* that reduce I_{CaL} were recently associated with the Brugada syndrome in concurrence with a short QT duration.[16]

At sites of local activation delay, the current available for excitation is modulated by currents activated after the upstroke of the action potential such as I_{to}[17] and I_{CaL}.[11,18,19] Therefore, we established experimentally whether excitation failure by current-to-load mismatch results in ST segment elevation on a pseudo-ECG in porcine epicardial shavings with introduced structural discontinuities. Second, we determined whether the Brugada ECG pattern by current-to-load mismatch is modulated by I_{to} and I_{CaL} in a computer model encompassing the heart and thorax.

Methods

The experimental protocol complied with the *Guide for the Care and Use of Laboratory Animals* published by the U.S. National Institutes of Health and was approved by the institutional animal experiments committee.

Epicardial shavings

Eight male pigs (25–35 kg) were premedicated with an intramuscular injection of ketamine (10–15 mg/kg, Animal Health BV, Bladel, The Netherlands) and midazolam (1.0 mg/kg, F. Hoffmann, La Roche Ltd., Basel, Switzerland). After induction of anesthesia with pentobarbital (20 mg/kg IV, CEVA Santé Animale, La Ballastière, France) and heparin (Leo Pharma BV, Breda, The Netherlands), VF was induced by a DC current, and the heart was removed and rapidly placed in ice-cold modified Tyrode's solution (NaCl 128 mmol/L, KCl 4.7 mmol/L, $CaCl_2$ 1.5 mmol/L, $MgCl_2$ 0.7 mmol/L, $NaHCO_3$ 28 mmol/L, NaH_2PO_4 0.5 mmol/L, glucose 11.0 mmol/L). Epicardial shavings (~30 × 20 × 0.5 mm) were cut with a dermatome parallel to the epicardial surface, while carefully avoiding regions containing the main coronary vasculature. Suitable preparations were immediately transferred to the superfusion setup and pinned to the wax floor of the perfusion chamber. The preparations were superfused (100 mL/min) with 0.5 L of recirculating modified Tyrode's solution at 37°C. The superfusate was gassed with 95% O_2/5% CO_2. Eleven preparations were used in this study. Three preparations were derived from the right ventricular free wall, and eight from the left ventricle. After determination of the fiber direction, isthmuses were created in a line parallel to the fiber orientation at ~6 mm intervals by puncturing of the epicardial shaving with two needles positioned at a fixed distance (either 0.9, 1.1, or 1.3 mm). After puncturing of the epicardial shavings, cuts were made parallel to the fiber direction away from the needles using an opthalmic scalpel. This technique allowed precise control over isthmus width (0.9, 1.1, or 1.3 mm). The preparations were then allowed to equilibrate for 1 hour.

Experimental setup

Preparations were stimulated at twice the diastolic threshold. A pseudo-ECG was recorded at 2 kHz from electrodes placed 5 mm from the epicardial shaving in the superfusion solution at either side of the preparation in a line perpendicular to the line of the isthmuses. The ECG electrode at the side of stimulation was the negative pole. Local activation was recorded either electrically (n = 4) or optically (n = 7). For electrical activation recording, two electrodes containing two silver wires were positioned on the epicardial surface of the epicardial shaving, one proximal and one distal to the isthmus. For the optical mapping, epicardial shavings were stained with di-4-ANEPPS 20 μmol/L (Invitrogen Corp., Carlsbad, CA) during 7.5 minutes and ± blebbistatin 10 μmol/L (Tocris Bioscience, Bristol, UK) was added to the modified Tyrode's solution to avoid mechanical artifacts caused by contraction. Fluorescence was obtained by exciting the stained tissue with a 5-W light emitting diode (cyan, 505 nm) reflected by a dichroic mirror and focused at the preparation through a tandem lens set. The emitted fluorescent light was transmitted through the tandem lens setup, filtered (>610 nm) and projected on a Micam Ultima optical camera (Scimedia USA Ltd., Costa Mesa, CA). The camera had 100 × 100 pixels and 1-kHz sampling frequency. The viewing window of the optical setup was 9 × 9 mm.

Recordings were made at varying basic cycle lengths (2000–200 ms) before and after addition of ajmaline 5 μmol/L (Solvay Pharmaceuticals GmbH, Hannover, Germany), a rate-dependent blocker of the cardiac sodium channel.[20] At baseline, the conduction velocity of the epicardial shavings was determined using activation maps during central stimulation at a cycle length of 500 ms. Preparations with successful conduction at baseline over the isthmuses at all tested frequencies were included in this study.

Data analysis

Data were analyzed using custom-made software based on MATLAB R2006b (MathsWorks Inc., Natick, MA).[21] Local electrograms or optical mapping data were aligned with the pseudo-ECG on the stimulation artifact.

The modulation of current-to-load mismatch by I_{to} and I_{CaL} in addition to ajmaline could not be tested in epicardial shavings because porcine ventricular cardiomyocytes do not express I_{to1}.[22] Furthermore, reduction of I_{CaL} reduces the action potential duration,[23] and this will increase the dia-

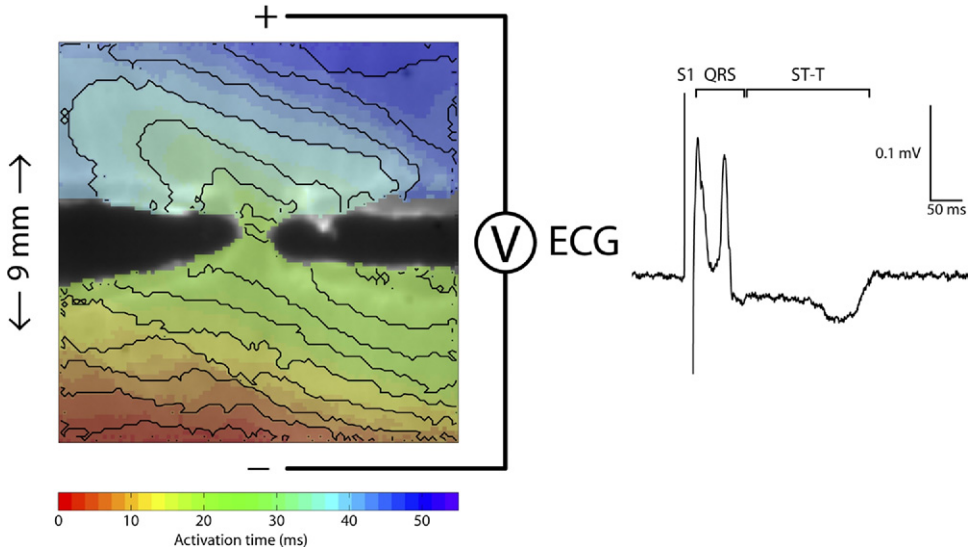

Figure 1 Optical map and pseudo-ECG of a porcine epicardial shaving after the introduction of isthmuses during stimulation from below. Colors correspond with local activation times, lines are 2.5-ms isochrones, viewing window is 9 × 9 mm. Tracing shows QRS complex and ST-T segment of the pseudo-ECG.

stolic interval during steady state pacing, which will affect the use-dependent blockade of the sodium channel by ajmaline. Therefore, we studied the effects of I_{to} and I_{CaL} in computer simulations.

Computer simulations

As before,[9] propagating action potentials were simulated with a whole-heart reaction-diffusion model containing 90 million nodes, each represented by a membrane model of the human ventricular myocyte.[24] Membrane ionic currents were computed with a human membrane model that included the differential characteristics of subendocardial, midmyocardial, and subepicardial myocytes.[25] Transmural fiber rotation was represented in the model. The ECG was computed using a bidomain model of the human heart and torso, including lungs and intracavitary blood volumes.[26] Structural discontinuities were simulated by the introduction of barriers (thickness 0.4–0.6 mm) in the outer 50% of the right ventricular wall. In these barriers, no intercellular coupling was present, but the interstitium was unaffected. The barriers contained gaps of 0.2 mm width in which the intercellular coupling was reduced to 30% of normal to mimic smaller gaps. Sodium channel conductivity (G_{Na}) was simulated at 100% or 30% of normal in the entire heart. The conductivity of the L-type calcium channels (G_{CaL}) was modified in steps from 50% to 400% of normal, and the conductivity of the transient outward channels (G_{to}) from 0% to 400% of normal in the entire heart. Simulation of a single cardiac beats in this model required 7–12 hours (SGI Altix computer, 128 processors).

Statistical analysis

The occurrence of conduction block after ajmaline was compared between groups of preparations with similar isthmus width using a Fisher's exact test. The level of statistical significance was set to $P<.05$.

Results

Epicardial shavings

At baseline, the conduction velocity of the epicardial shavings was 60.7 ± 5.7 cm/s longitudinal and 15.2 ± 3.7 cm/s (mean ± SD) transversal to the fiber direction. A typical example of an activation map and pseudo-ECG of an epicardial shaving after creation of an isthmus is shown in Figure 1.

After ajmaline, conduction blocked at the isthmuses in most of the preparations. The fraction of blocked beats was greater at shorter cycle lengths and in preparations with the smallest isthmus width (Figure 2). Total conduction block occurred in three of four preparations with isthmuses of 0.9 mm versus one of seven with isthmuses ≥1.1 mm ($P<.05$).

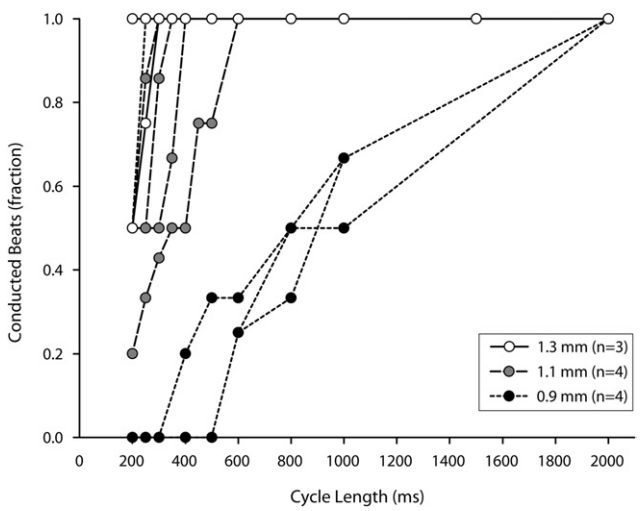

Figure 2 Graph showing the portion of beats conducted over the isthmuses in epicardial shavings at increasing pacing rates after ajmaline (5 μmol/L). The conduction block depended on the width of the isthmuses and on the pacing rate; n = no. of preparations.

No blocked beats at any cycle length were observed in two of three preparations with isthmuses of 1.3 mm versus eight of eight with isthmuses ≤1.1 mm ($P = .055$).

Figure 3 shows the activation maps, optically recorded action potentials, and pseudo-ECGs of two consecutive beats of an epicardial shaving containing three isthmuses (one outside the recording area) of 1.1 mm after ajmaline during stimulation at a cycle length of 300 ms. In the upper panel, conduction over one of the isthmuses is successful and the myocardium distal of the isthmuses was activated with a long delay. This resulted in a long fractionated QRS complex followed by a negative T wave on the pseudo-ECG. In the lower panel, conduction fails at both isthmuses, resulting in excitation failure of the myocardium distal of the isthmuses. Activation at the proximal site of the barrier gives rise to a potential gradient over the isthmuses and current flow toward the positive ECG electrode, which is seen as ST segment elevation on the pseudo-ECG.

Computer simulations

Local activation

All simulations were run with a model of both ventricles. Three-dimensional activation maps of a subepicardial section of this model after introduction of subepicardial structural discontinuities are shown in Figure 4. For clarity, the structural discontinuities were made transparent. Graphs below show local action potentials; I_{Na}, I_{to}, and I_{CaL}; and the total current given or received through the gap junctions at four different locations indicated in the activation maps. At baseline (Figure 4A), activation is delayed at the distal end of the isthmuses, but all myocardium distal from the isthmuses reached threshold potential and was activated. As shown before,[9] reduction of the

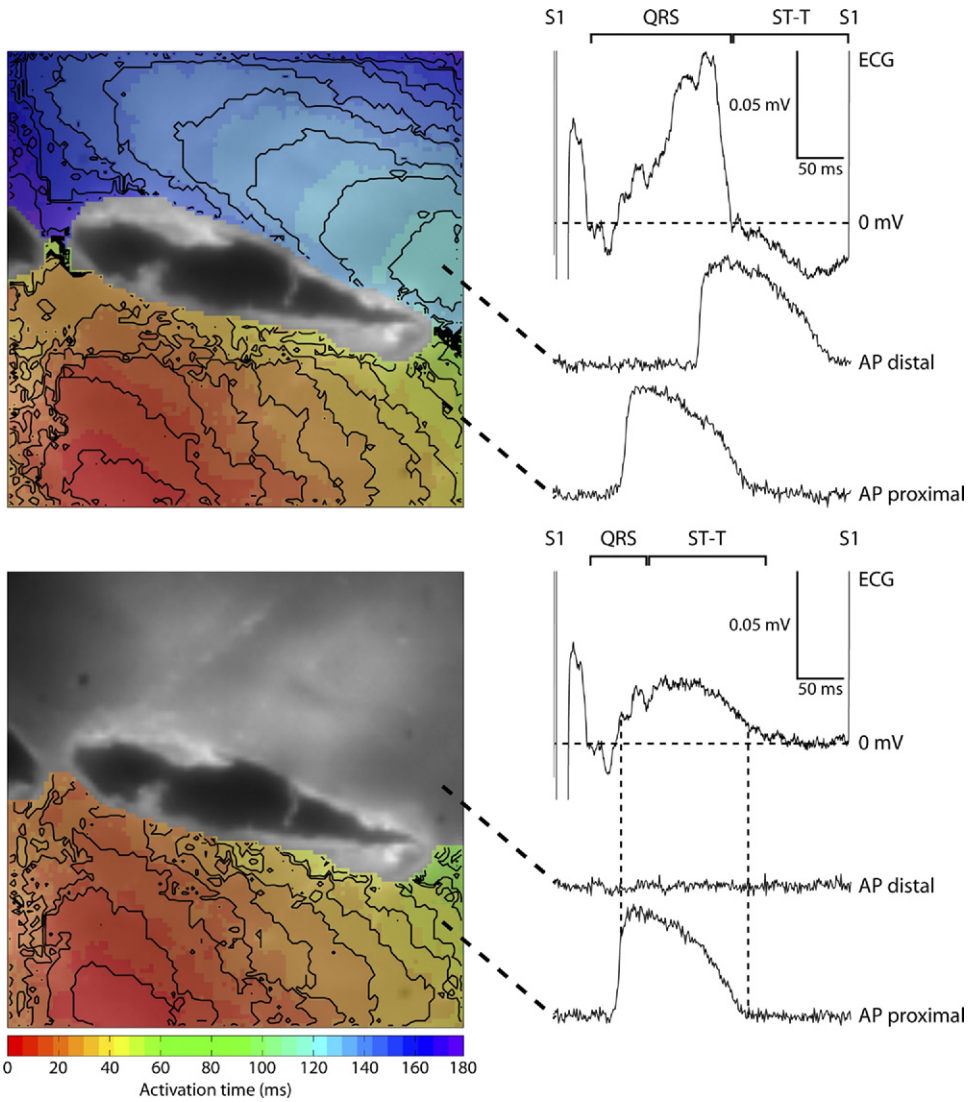

Figure 3 Activation maps showing two out of three isthmuses of 1.1 mm width of an epicardial shaving, optically recorded action potentials, and pseudo-ECGs of two consecutive beats after ajmaline during stimulation at a cycle length of 300 ms. In the upper panel, conduction over the right isthmus was successful and the myocardium distal of the isthmus was activated late, resulting in a long QRS duration followed by a negative T wave on the pseudo-ECG. In the lower panel, conduction failed at all isthmuses, resulting in excitation failure of the myocardium distal of the isthmuses and in a potential gradient over the isthmuses, which is seen as ST segment elevation on the pseudo-ECG. Colors correspond with local activation; lines are 5-ms isochrones; viewing window is 9 × 9 mm; and S1 indicates the stimulation artifact, QRS complex, and ST-T segment of the pseudo-ECG.

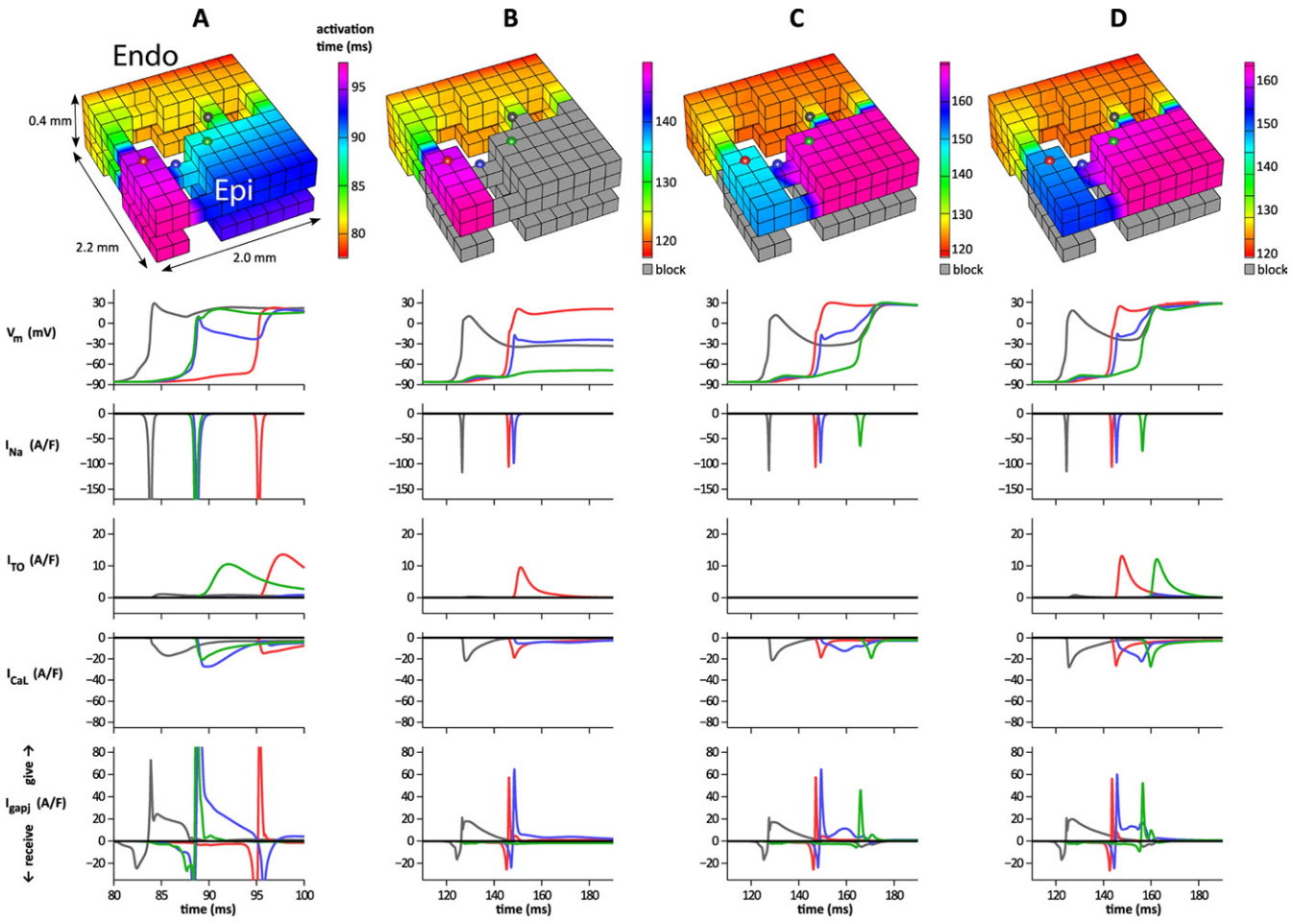

Figure 4 Three-dimensional activation map of a subepicardial section of the computer model after introduction of subepicardial structural discontinuities and graphs showing action potentials and ion currents at four locations, which are indicated by colored spheres in the activation map. At baseline (**A**), activation is delayed at the distal end of the isthmuses. However, all distal myocardium is activated. After reduction to 30% of the conductance of the cardiac sodium channel (**B**), activation is blocked at the isthmuses and subepicardial sites failed to excite. After reduction of the conductance of the transient outward current to 0% of normal (**C**), the phase 1 repolarization at subepicardial locations is reduced (red) and more current is provided to sites distal of the isthmus (green), and excitation threshold potential is reached. Likewise, an increase in the L-type calcium current to 150% of normal (**D**) resulted in a higher depolarizing current being provided to the location distal of the isthmuses (green) and prevented excitation failure. Colors in the activation map correspond with local activation time. Endo indicates the endocardial side and epi the epicardial side of the section. In panels A and D, I_{to} at the gray marker is small, because it is located in endocardial tissue, where the expression of I_{to} is relatively low.

conductance of the cardiac sodium channel to 30% of normal (Figure 4B) resulted in activation block at some of the isthmuses and in excitation failure in part of the subepicardial tissue distal to the isthmuses. Reduction of the conductance of G_{to} to 0% of normal (Figure 4C) prevented subepicardial excitation failure at some sites. Phase 1 repolarization at subepicardial locations was reduced (see red action potential), and more current was provided to sites distal to the isthmus (green), which enabled it to reach threshold potential and prevented subepicardial excitation failure. Likewise, an increase in G_{CaL} to 150% of normal (Figure 4D) resulted in a higher depolarizing current being provided to the location distal of the isthmuses (green) and prevented excitation failure.

Simulated ECGs

The subepicardial activation delay and excitation failure after reduction of G_{Na} to 30% in structurally discontinuous heart resulted in ST segment elevation followed by a negative T wave in the right precordial leads of the ECG. The percentage of elements of the entire heart that failed to excite and the right precordial ST segment elevation after G_{Na} reduction were modulated by G_{to} and G_{CaL}. An increase of G_{to} (Figure 5) or a reduction of G_{CaL} (Figure 6) resulted in more sites that failed to excite and in greater amplitude of the right precordial ST segment elevation. Conversely, a reduction of G_{to} or an increase of G_{CaL} improved the success of conduction, decreased the number of sites that failed to excite, and reduced the amplitude of the right precordial ST segment elevation. The same changes in G_{to} and G_{CaL} did not result in ST segment deviation in the heart without structural discontinuities either at normal G_{Na} or after reduction of G_{Na} to 30% of normal (data not shown).

Discussion

In this study, we directly demonstrated that excitation failure by current-to-load mismatch results in ST segment ele-

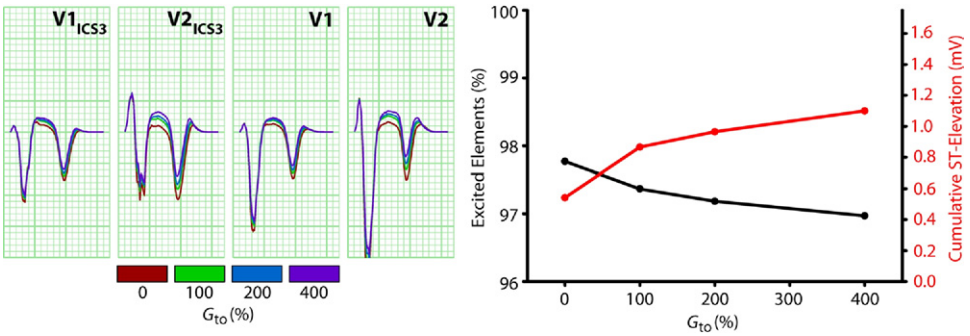

Figure 5 Simulated ECGs of the heart with structural discontinuities and reduced sodium current at different levels of conductivity of the channel underlying the transient outward current (G_{to}). The graphs on the right relate the corresponding percentage of excited elements of the whole heart with the cumulative ST segment elevation in the four right precordial leads. G_{to} modulated success of conduction in structurally discontinuous right ventricular subepicardium. Reduction of G_{to} prevented excitation failure at some subepicardial sites and decreased the right precordial ST segment elevation on the ECG. $V1_{ICS3}$ and $V2_{ICS3}$ indicate leads V1 and V2 positioned in the third intercostal space.

vation on the ECG. In porcine epicardial shavings, success of conduction across an isthmus depended on the width of the isthmus and on the available I_{Na}, which was varied by addition of the rate-dependent sodium channel blocker ajmaline and by changing the pacing frequency. Small isthmuses ($\leq$ 1.1 mm) in combination with reduced sodium current resulted in excitation failure and ST segment elevation on the pseudo-ECG. Additionally, we demonstrated in a computer model that I_{to} and I_{CaL} modulate the excitation failure-induced Brugada ECG pattern in discontinuous myocardium. At sites of sudden expansion of the myocardium, a small source volume must activate a large sink volume. This caused activation delay and made the success of conduction sensitive to currents activated shortly after the upstroke of the action potential, such as I_{to} and I_{CaL}. The repolarizing I_{to} reduced, and the depolarizing I_{CaL} increased the current available for downstream depolarization and success of conduction.

These results are in line with clinical observations in patients with Brugada syndrome. Subtle signs of structural discontinuities in histological studies,[8] imaging studies,[5] and electrophysiological studies[6,7] are common in patients with Brugada syndrome. Additionally, enhancement of I_{CaL} by isoproterenol can reduce the Brugada ECG pattern[3] and can suppress electrical storms.[15] Likewise, blockade of I_{to} by quinidine can reduce the ST segment elevation[13] and lower the inducibility of arrhythmias.[14] In a case report, Watanabe et al. have demonstrated that quinidine reversibly eliminated late potentials on the signal-averaged ECG of a patient with Brugada syndrome.[27] Therefore, the observation that the Brugada syndrome is modulated by I_{to} and I_{CaL} is consistent with the hypothesis that conduction disturbances by current-to-load mismatch cause the Brugada ECG pattern.

As shown schematically in Figure 7, current-to-load mismatch can cause unidirectional conduction block depending on the distribution of structural discontinuities and the depolarizing current available for conduction. The first observed extrasystole can be caused by reentrant activation. The ventricular arrhythmias associated with the Brugada ECG pattern can therefore be explained by current-to-load mismatch without the need for an extrasystole by a focal mechanism.

The question remains whether excitation failure by current-to-load mismatch can also underlie the ST segment elevation and ventricular fibrillation in other patient groups. Haïssaguerre et al. have demonstrated that elevation of the QRS-ST

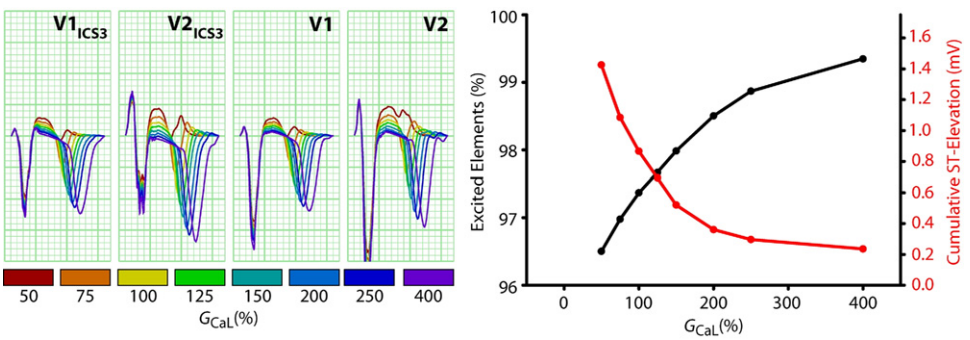

Figure 6 Simulated ECGs of the heart with right ventricular structural discontinuities and reduction of the cardiac sodium current at different levels of conductivity of the L-type calcium channel (G_{CaL}). The graphs on the right relate the corresponding percentage of excited elements of the whole heart with the cumulative ST segment elevation in the four right precordial leads. G_{CaL} modulated success of conduction in structurally discontinuous right ventricular subepicardium. Increased G_{CaL} prevented excitation failure at some subepicardial sites and decreased the right precordial ST segment elevation on the ECG.

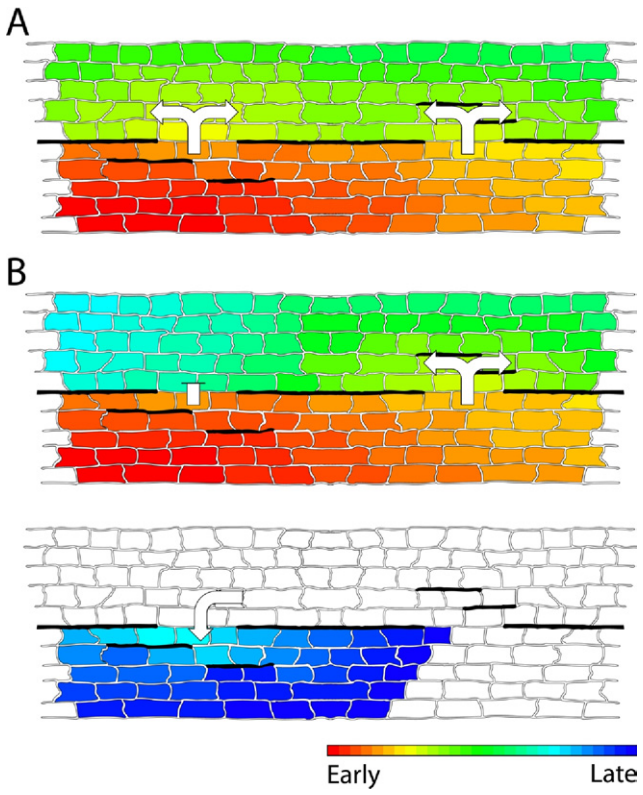

Figure 7 Schematic drawings illustrating the induction of reentrant arrhythmias by current-to-load mismatch in myocardium containing two isthmuses. **A:** During normal conditions, the redundancy in excitatory current makes conduction successful over both isthmuses and there is no reentrant activation. **B:** A reduction of the cardiac sodium current or L-type calcium current or an increase of the transient outward current lowers the excitatory current and can cause unidirectional conduction block depending on the local geometry of the myocardium. In the top drawing, activation is blocked at the left but not at the right isthmus. The asymmetrical distribution of the structural discontinuities at the left isthmus make conduction in the opposite direction successful, and activation reenters the proximal myocardium. Colors depict activation time; black indicates fibrous tissue between myocardium.

junction on the inferior and lateral leads (also termed inferolateral early-repolarization sign [ERS]) is associated with idiopathic VF and that these patients are at high risk of recurrent VF.[28] As in the Brugada syndrome, isoproterenol[28,29] and quinidine[29] reduce or eliminate inferolateral ERS and may prevent arrhythmias in these patients.[29,30] Furthermore, inferolateral ERS is a common feature in patients with Brugada syndrome,[31] and sodium channel blockade can provoke the Brugada ECG pattern in inferior or lateral leads in ~5% of patients with Brugada syndrome.[30] However, sodium channel blockade, the most potent modulator of the Brugada ECG pattern, usually has no effect on inferolateral ERS.[30,31] Despite these similarities, the mechanisms of ST segment elevation in patients with the Brugada syndrome and in those with inferolateral ERS are therefore likely different but share modulation by I_{to} and I_{CaL}.

Study limitations

Variation of I_{to} and I_{CaL} was only performed in the computer model of the Brugada syndrome and not in epicardial shavings. However, others have provided ample demonstration of the effects of I_{to}[17] and I_{CaL}[11,19,32] on the success of conduction in the setting of local activation delay. Furthermore, the width of the isthmuses in epicardial shavings that resulted in conduction block in the present study as well as in previous reports[33] was larger than those in the computer model. To obtain conduction block by current-to-load mismatch in a computer model with isthmus sizes comparable to those of the epicardial shavings, it may be necessary to account for the discontinuities at the cellular level.[34] With the currently available computing power, this is not feasible for a whole-heart model. In addition, the cutting of the epicardial shavings may have changed the interstitial conductivity. Because the nature and size of these changes are unknown, they were not accounted for in the computer model.

Conclusions

Excitation failure by current-to-load mismatch causes ST segment elevation and, like ST segment elevation in Brugada patients, is modulated by I_{Na}, I_{to}, and I_{CaL} . Therefore, current-to-load mismatch may underlie the Brugada syndrome.

Acknowledgments

The authors thank Charly Belterman and Goos Huijzer for invaluable assistance.

References

1. Brugada P, Brugada J. Right bundle branch block, persistent ST segment elevation and sudden cardiac death: a distinct clinical and electrocardiographic syndrome. A multicenter report. J Am Coll Cardiol 1992;20:1391–1396.
2. Hoogendijk MG, Opthof T, Postema PG, Wilde AAM, de Bakker JMT, Coronel R. The Brugada ECG pattern: a marker of channelopathy, structural heart disease, or neither? Toward a unifying mechanism of the Brugada syndrome. Circ Arrhythm Electrophysiol 2010;3:283–290.
3. Miyazaki T, Mitamura H, Miyoshi S, Soejima K, Ogawa S, Aizawa Y. Autonomic and antiarrhythmic drug modulation of ST segment elevation in patients with Brugada syndrome. J Am Coll Cardiol 1996;27:1061–1070.
4. Priori SG, Napolitano C, Gasparini M, et al. Natural history of Brugada syndrome: insights for risk stratification and management. Circulation 2002;105:1342–1347.
5. Catalano O, Antonaci S, Moro G, et al. Magnetic resonance investigations in Brugada syndrome reveal unexpectedly high rate of structural abnormalities. Eur Heart J 2009;30:2241–2248.
6. Ikeda T, Sakurada H, Sakabe K, et al. Assessment of noninvasive markers in identifying patients at risk in the Brugada syndrome: insight into risk stratification. J Am Coll Cardiol 2001;37:1628–1634.
7. Postema PG, van Dessel PFHM, de Bakker JMT, et al. Slow and discontinuous conduction conspire in Brugada syndrome: a right ventricular mapping and stimulation study. Circ Arrhythm Electrophysiol 2008;1:379–386.
8. Zumhagen S, Spieker T, Rolinck J, et al. Absence of pathognomonic or inflammatory patterns in cardiac biopsies from patients with Brugada syndrome. Circ Arrhythm Electrophysiol 2009;2:16–23.
9. Hoogendijk MG, Potse M, Linnenbank AC, et al. Mechanism of right precordial ST-segment elevation in structural heart disease: excitation failure by current-to-load mismatch. Heart Rhythm 2010;7:238–248.
10. de la Fuente D, Sasyniuk B, Moe GK. Conduction through a narrow isthmus in isolated canine atrial tissue: a model of the W-P-W syndrome. Circulation 1971;44:803–809.
11. Inoue H, Zipes DP. Conduction over an isthmus of atrial myocardium in vivo: a possible model of Wolff-Parkinson-White syndrome. Circulation 1987;76:637–647.
12. Stanton MS. Class 1 antiarrhythmic drugs: quinidine, procainamide, disopyramide, lidocaine, mexiletine, tocainide, phenytoin, morcizine, flecainide, propafenone. In: Zipes DP, Jalife J, eds. Cardiac electrophysiology: from cell to bedside. Philadelphia, PA: WB Saunders Company, 2000:890–903.

13. Alings M, Dekker LRC, Sadee A, Wilde AAM. Quinidine induced electrocardiographic normalization in two patients with Brugada syndrome. Pacing Clin Electrophysiol 2001;24:1420–1422.
14. Belhassen B, Viskin S, Fish R, Glick A, Setbon I, Eldar M. Effects of electrophysiologic-guided therapy with class IA antiarrhythmic drugs on the long-term outcome of patients with idiopathic ventricular fibrillation with or without the Brugada syndrome. J Cardiovasc Electrophysiol 1999;10:1301–1312.
15. Tanaka H, Kinoshita O, Uchikawa S, et al. Successful prevention of recurrent ventricular fibrillation by intravenous isoproterenol in a patient with Brugada syndrome. Pacing Clin Electrophysiol 2001;24:1293–1294.
16. Antzelevitch C, Pollevick GD, Cordeiro JM, et al. Loss-of-function mutations in the cardiac calcium channel underlie a new clinical entity characterized by ST-segment elevation, short QT intervals, and sudden cardiac death. Circulation 2007;115:442–449.
17. Huelsing DJ, Spitzer KW, Cordeiro JM, Pollard AE. Conduction between isolated rabbit Purkinje and ventricular myocytes coupled by a variable resistance. Am J Physiol Heart Circ Physiol 1998;274:H1163–H1173.
18. Joyner RW, Kumar R, Wilders R, et al. Modulating L-type calcium current affects discontinuous cardiac action potential conduction. Biophys J 1996;71:237–245.
19. Rohr S, Kucera JP. Involvement of the calcium inward current in cardiac impulse propagation: induction of unidirectional conduction block by nifedipine and reversal by Bay K 8644. Biophys J 1997;72:754–766.
20. Heistracher P. Mechanism of action of antifibrillatory drugs. Naunyn Schmiedebergs Arch Pharmacol 1971;269:199–212.
21. Potse M, Linnenbank AC, Grimbergen CA. Software design for analysis of multichannel intracardial and body surface electrocardiograms. Comput Methods Programs Biomed 2002;69:225–236.
22. Li GR, Du XL, Siow YL, O K, Tse HF, Lau CP. Calcium-activated transient outward chloride current and phase 1 repolarization of swine ventricular action potential. Cardiovasc Res 2003;58:89–98.
23. Vitek M, Trautwein W. Slow inward current and action potential in cardiac Purkinje fibres. Pflugers Arch 1971;323:204–218.
24. Potse M, Dubé B, Richer J, Vinet A, Gulrajani RM. A comparison of monodomain and bidomain reaction-diffusion models for action potential propagation in the human heart. IEEE Trans Biomed Eng 2006;53:2425–2435.
25. ten Tusscher KHWJ, Noble D, Noble PJ, Panfilov AV. A model for human ventricular tissue. Am J Physiol Heart Circ Physiol 2004;286:H1573–H1589.
26. Potse M, Dubé B, Vinet A. Cardiac anisotropy in boundary-element models for the electrocardiogram. Med Biol Eng Comput 2009;47:719–729.
27. Watanabe H, Chinushi M, Osaki A, et al. Elimination of late potentials by quinidine in a patient with Brugada syndrome. J Electrocardiol 2006;39:63–66.
28. Haïssaguerre M, Derval N, Sacher F, et al. Sudden cardiac arrest associated with early repolarization. N Engl J Med 2008;358:2016–2023.
29. Haïssaguerre M, Sacher F, Nogami A, et al. Characteristics of recurrent ventricular fibrillation associated with inferolateral early repolarization: role of drug therapy. J Am Coll Cardiol 2009;53:612–619.
30. Sarkozy A, Chierchia GB, Paparella G, et al. Inferior and lateral electrocardiographic repolarization abnormalities in Brugada syndrome. Circ Arrhythm Electrophysiol 2009;2:154–161.
31. Letsas KP, Sacher F, Probst V, et al. Prevalence of early repolarization pattern in inferolateral leads in patients with Brugada syndrome. Heart Rhythm 2008;5:1685–1689.
32. Shaw RM, Rudy Y. Ionic mechanisms of propagation in cardiac tissue: roles of the sodium and L-type calcium currents during reduced excitability and decreased gap junction coupling. Circ Res 1997;81:727–741.
33. Cabo C, Pertsov AM, Baxter WT, Davidenko JM, Gray RA, Jalife J. Wave-front curvature as a cause of slow conduction and block in isolated cardiac muscle. Circ Res 1994;75:1014–1028.
34. Spach MS, Miller WT, III, Dolber PC, Kootsey JM, Sommer JR, Mosher CE, Jr.The functional role of structural complexities in the propagation of depolarization in the atrium of the dog. Cardiac conduction disturbances due to discontinuities of effective axial resistivity. Circ Res 1982;50:175–191.